EM Simulations of Super-Resolution With the Active Surface of a Radio Telescope

Luca Olmi and Pietro Bolli

Abstract – The concept of super-resolution refers to various methods for improving the angular resolution of an optical imaging system beyond the classical diffraction limit. A feasible method to design antennas and telescopes with angular resolution better than the diffraction limit consists of using variable-transmittance pupils. The simplest transmittance pupils are binary phase-shift masks, also known as Toraldo pupils, consisting of finite-width concentric coronae which modify the phase of the incident wavefront. In principle, the active surface of a radio telescope could be used to modify the wavefront in the same way as a Toraldo pupil. In order to study the feasibility of this technique, in this work we describe a method, based on EM numerical simulations, to analyze the antenna point spread function when different types of active surfaces and focal positions are used.

1. Introduction

The concept of super-resolution (SR) refers to various methods for improving the angular resolution of an optical imaging system beyond the classical diffraction limit. In optical microscopy, several techniques have already been developed with the aim of narrowing the central lobe of the illumination point spread function (PSF). However, microscopy SR techniques cannot be easily applied to astronomical instrumentation, and thus few efforts have been made to overcome the diffraction limit of filled-aperture telescopes.

Variable-transmittance pupils represent one viable approach to achieving SR in radio astronomy. Toraldo di Francia suggested in 1952 [1] that the classical limit of optical resolution could be improved interposing a filter consisting of finite-width concentric annuli of different amplitude and phase transmittance at the entrance pupil of an optical system, now also known as Toraldo pupils (TPs). The original analytical description of the TP given by Toraldo di Francia assumed an ideal optical system where, for example, the transmittance filters are infinitely thin and an ideal source is assumed that achieves both the required amplitude apodization and uniform phase illumination over the pupil.

However, any practical realization of a TP in the microwave range cannot operate under such ideal constraints, and thus, as part of the Pupille Toraldo project (http://www.ifac.cnr.it/PUTO/), we have experimentally verified that a simple TP can work even under less-than-ideal conditions. Our measurements demonstrated that the SR effect is achieved with both three- and four-coronae TPs, and also showed good agreement with previously conducted EM simulations using the FEKO software tool. (http://www.altairhyperworks.com/product/FEKO) [2].

Manuscript received 28 July 2020.

Luca Olmi and Pietro Bolli are with the Istituto Nazionale di Astrofisica (INAF), Osservatorio Astrofisico di Arcetri, Largo E. Fermi 5, I-50125 Firenze, Italy; e-mail: olmi.luca@gmail.com, pbolli@arcetri.inaf.it.

2. Implementation of a TP System on a Radio Telescope

Although diffraction from an isolated TP, illuminated by a plane wave, shows the SR effect, the question arises how to combine the pupil together with other optical components so that an imaging system can also operate in SR mode. Ideally, the TP should be placed at the entrance pupil of the telescope (i.e., at the aperture plane of the primary reflector). However, an easier and more accessible location is at the exit pupil of the telescope.

Since every modification of the incoming wavefront at the exit pupil is equivalent to the same modification applied at the entrance pupil, we have designed a TP optical module based on a two-lens collimator placed after the Cassegrain focus and before the receiver dewar [3]. EM simulations and laboratory measurements of the collimator, showing the SR effect, are described elsewhere [3]. EM simulations and preliminary field tests of the collimator mounted on a test satellite antenna have also shown that SR can be achieved with this optical arrangement [4].

On the other hand, the amplitude and phase distribution on plane apertures of reflector antennas can be controlled through “surface shaping” or actively controlled surfaces. The pioneering work of Galindo [5] showed how to use the shaping technique to achieve arbitrary phase and amplitude distributions over the main aperture of reflector antennas, and since then this technique has been used to improve antenna aperture efficiency, side-lobe levels, cross-polarization levels, and so on. Active compensation of the antenna deformations is a more recent achievement in radio astronomy, and it is currently used on large radio telescopes to adjust the antenna structure and shape to reduce the loss of electric performance caused by various environmental effects (see, e.g., [6]).

To our knowledge, neither of these two techniques has been used so far to mimic the behavior of an ideal TP placed at the aperture plane of a reflector antenna [7]. Since two of the radio telescopes operated by the Italian National Institute for Astrophysics (http://www.inaf.it)—the Noto telescope and the Sardinia Radio

Telescope (SRT; https://www.ira.inaf.it/Radiotelescopes.html)—are provided with an active primary surface, it is of interest to analyze whether the active surface of a radio telescope could be used to implement the SR effect. In this work we apply our analysis to the Noto antenna, which has a classical Cassegrain design; we leave the analysis of the SRT, which has a more complex-shaped design, for a later article.

The use of the active surface to achieve the SR effect would in principle present several advantages compared to the collimator + TP optical configuration. First, the required binary phase shifts are introduced using a properly modified reflecting surface, rather than a 3-D TP in transmission using standard dielectric material, which can induce significant losses. A second advantage is that no modification inside the receiver cabin is required, as would be the case if a TP optical module were to be installed near the secondary focus and in front of the receiver dewar window. A third advantage is that the active surface can be adjusted to work with any available receiver, whereas a separate collimator would have to be fabricated for each receiver. However, depending on the specific active surface, there are also a number of problems with this technique, which we describe in the next section.

3. Simulating a TP With an Active Primary Reflector

3.1. Feasibility of the Method

In order to test whether the method we have outlined is really feasible to achieve the SR effect on a radio telescope, we first performed a series of preliminary EM simulations using the superposition technique. The numerical simulations have been carried out using the GRASP software tool (https://www.ticra.com/software/grasp/), and as an initial test bed (requiring little computation time) we have used a 9 m parabolic reflector with a focal ratio of $F = 3$, approximately the same as the Medicina and Noto 32 m antennas at their Cassegrain focus.

The EM simulations were carried out in reception mode, assuming an incident plane wave, and we computed separately the complex fields generated at the focus by each annular section of the antenna corresponding to the geometry of a three-corona TP (TP3) projected on the reflector surface, selected using the appropriate radial range.

Applying the superposition technique, the three separate fields were summed to obtain the total intensity at the focus of the reflector. The intensities resulting from the individual fields and their complex (in-phase) sum are shown in Figure 1; the bottom panel shows that the total intensity reconstructed from the summed fields is practically identical to the intensity obtained by GRASP using the full aperture of the antenna.

We have recently used this method to simulate TP3 geometry projected on the aperture plane of the

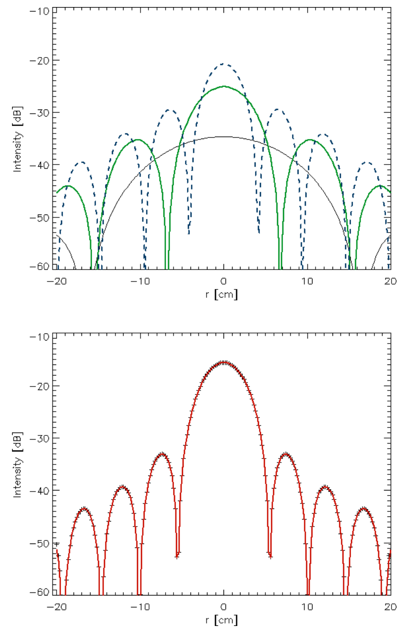

Figure 1. (Top) Simulated PSFs at the focus of a 9 m diameter, $F = 3$ paraboloid using GRASP. The intensities of the individual fields generated by each of three separate coronae are shown. (Bottom) Black "+" signs represent the intensity corresponding to the complex sum of the individual fields shown in the top panel; the solid red curve represents the PSF obtained from the whole 9 m antenna.

antenna [7]. Once again, the total field at the focus was reconstructed through the complex sum of the individual fields, but this time a 180° phase shift was artificially introduced to the field emanating from the central corona.

We have shown that using this technique, the SR effect can be obtained, accompanied by both a narrower main lobe and higher side lobes, as expected [7]. Furthermore, in our preliminary test no visible difference was obtained when the phase delay was applied through a physical displacement of the surface compared to the ideal case of a phase delay applied in the aperture plane of the antenna.

3.2. EM Simulations at the Noto Primary Focus

The Noto active primary surface consists of a total of 248 panels distributed along six separate rings. The two innermost rings of panels are fixed, while the four remaining rings are composed of active panels (see top panel of Figure 2). In order to limit the complexity and extra weight of the actuator network, 244 actuators are used, with each one positioned at the corners of four panels. Therefore, each actuator operates on four panels simultaneously (see bottom panel of Figure 2).

The primary active reflector can be shaped to resemble a TP by displacing the appropriate rings of panels. The geometry of the baseline TP that can be implemented with the active surface is limited by the number of panel rings and the size of the individual panels. Therefore, in this preliminary study we discuss

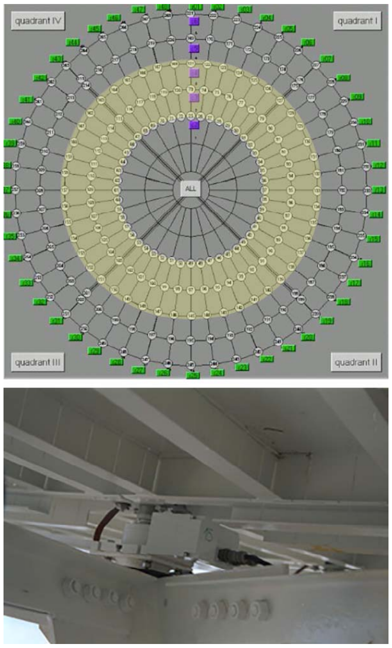

Figure 2. (Top) Distribution of the actuators on the active surface of the Noto 32 m antenna. The yellow-shaded area corresponds to the panels that need to be shifted to mimic the TP3 geometry of Olmi and Bolli [7]. (Bottom) The corners of four distinct panels connected to a single actuator.

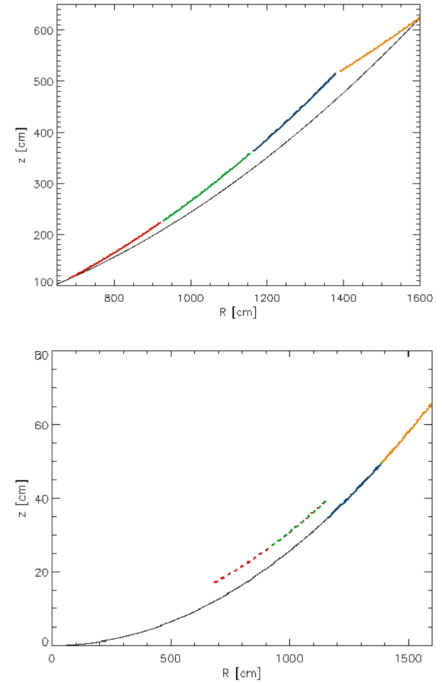

Figure 3. (Top) Radial profile of a zoomed section of the Noto primary reflector. The colored arcs represent the positions of the active panels when rings 2 and 3 are shifted to achieve a TP3-like geometry. (Bottom) Radial profile of the Noto equivalent parabola with rings 1 and 2 (red and green, dashed) shifted along the optical axis and rings 3 and 4 left unchanged (panel displacement has been exaggerated for better visibility).

the implementation of a simple TP3 which can be approximated using the limited number and geometry of the active rings of panels. One possible choice is shown in Figure 2, where it can be seen that the corona inducing the 180° phase delay covers active rings 1 and 2.

In order to test the performance of the modified active surface, we carried out EM simulations at the primary and Cassegrain foci of the antenna. In the latter case, as a first step we used the equivalent paraboloid, since the EM simulations were easier to implement and less time-consuming. However, in this case it is implicitly assumed that although the radial distances at which the actuators are placed are the same, the shapes of the (virtual) individual panels on the equivalent parabola are indeed different from the real ones.

In order to reproduce on the primary reflector the geometry of the TP3 shown in Figure 2, the rings of panels 1 and 2 must induce the 180° phase delay on the incoming wavefront. In the ideal case, if the panels had all degrees of freedom, this would be achieved by translating all panels in these specific rings in a direction parallel to the optical axis (or z axis) so that the incoming rays, upon reflection on the shifted panels, would be subject to a difference in the optical path equal to $\lambda/2$ as compared to the unaffected rays (see Figure 3). However, because each actuator is attached to four panels, the displacement in one ring of panels actually induces partial rotation of the adjacent rings (see next section). Figure 3 illustrates this effect, and shows how the equivalent parabola is much “shallower” compared to the true shape of the primary reflector.

For the purpose of simulating the fields at the primary focus, we will assume for the moment that each panel can move independently from the others, and we will come back to the real actuator configuration later. The top panel of Figure 4 shows the resulting radial cut of the PSF at the primary focus of the Noto antenna. The figure shows the unmodified surface and the surface when the rings of panels 1 and 2 are shifted to introduce the 180° phase delay, as already described.

We note that both PSFs in the top panel of Figure 4 are almost identical—that is, no SR is introduced by the modified active surface. This is a direct consequence of introducing the phase delay through a modification to the *curved* reflecting surface, rather than applying it in the aperture plane, as we did in our preliminary tests (see Section 3.1). In fact, by shifting one or more rings of panels, we introduce two additional optical effects: first, the phase delay is introduced through a deformation of the ideal geometrical profile, which in turn introduces unwanted optical aberrations. Second, the differences in optical path of the incoming rays from a direction parallel to the optical axis, upon reflection on the shifted panels, are not all equal to $\lambda/2$ as compared to the unaffected rays. This is because panels are curved, rather than flat, and this effect is more significant at low $f/\#$, such as at the primary focus.

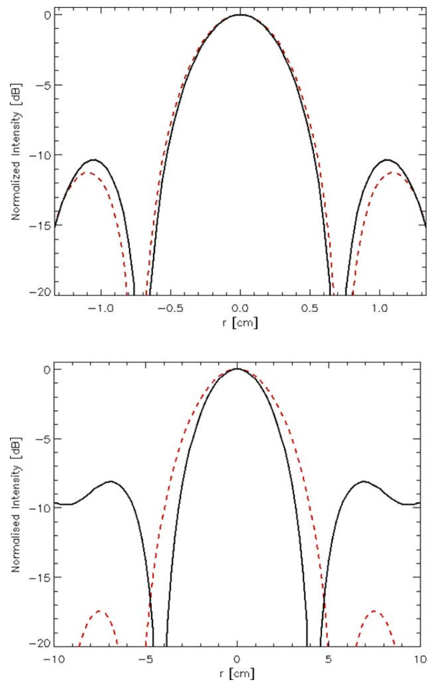

Figure 4. (Top) Simulated PSFs at the primary focus of the Noto antenna using GRASP. The PSF of the nominal, unmodified reflector surface is shown by the dashed red line. The solid black line shows the resulting PSF when the active surface is modified according to the TP3 geometry. (Bottom) Same as the top, but at the focus of the equivalent paraboloid of the Noto antenna.

3.3 EM Simulations With the Noto Equivalent Parabola

We then repeated our simulations, replacing the primary reflector with the equivalent parabola of the Noto antenna. The radial profile (r,z) of the modified equivalent parabola was imported in GRASP, and then the EM simulations were performed using the same method described in Section 3.1. The bottom panel of Figure 4 shows a radial cut of the PSF of both the unmodified surface and the TP3-equivalent surface, and the SR effect is clearly visible.

For the next step of this analysis we withdrew the assumption of the ideal active surface, where panels have fully independent movements. In the real active surface, each actuator (except those at the edges of the active surface) operates on *two* rings of panels simultaneously. As a consequence, adjusting the surface to mimic the TP3 geometry causes some of the panels to undergo a partial rotation (around an axis perpendicular to the plane of Figure 3) instead of a pure translation along the z-axis, as in the ideal model. Therefore, the mechanical coupling between adjacent rings of panels prevents the active surface from reshaping exactly as required by, in our case, a TP3 geometry, and our EM simulations show that the SR effect is washed out completely.

We expect the situation to be different for the active surface of the SRT, which consists of 1116 actuators, with the active panels distributed according to 96 radial lines and 14 rings. The major advantage compared to the Noto antenna is the much larger number of rings with active panels, providing a better spatial resolution as far as the ability to modify the geometry of the surface is concerned. On the other hand, both primary and secondary reflectors of the SRT are "shaped" surfaces, and thus modifications to the active surface of the primary reflector might have undesired effects on the final optical performance.

4. References

1. G. Toraldo di Francia, "Super-Gain Antennas and Optical Resolving Power," Il Nuovo Cimento (Suppl.), 9, 1952, p. 426-435.
2. L. Olmi, P. Bolli, L. Cresci, F. D'Agostino, M. Migliozzi, et al., "Laboratory Measurements of Super-Resolving Toraldo Pupils for Radio Astronomical Applications," *Experimental Astronomy*, **43**, 2017, pp. 285-309.
3. L. Olmi, P. Bolli, L. Carbonaro, L. Cresci, P. Marongiu, et al., "Design and Test of a Toraldo Pupil Optical Module for the Medicina Radio Telescope," 2018 2nd URSI Atlantic Radio Science Meeting (AT-RASC), Meloneras, Spain, May-June 2018, pp. 1-4. Publisher: IEEE.
4. L. Olmi, P. Bolli, L. Carbonaro, L. Cresci, A. Donati, et al., "Simulations and Tests of a Super-Resolving Optical Module Using a Satellite Antenna," 2019 23rd International Conference on Applied Electromagnetics and Communications (ICECOM), Dubrovnik, Croatia, September-October 2019, pp. 1-4. Publisher: IEEE.
5. V. Galindo, "Design of Dual-Reflector Antennas with Arbitrary Phase and Amplitude Distributions," *IEEE Transactions on Antennas and Propagation*, **12**, 4, July 1964, pp. 403-408.
6. C. Wang, H. Li, K. Ying, Q. Xu, N. Wang, et al., "Active Surface Compensation for Large Radio Telescope Antennas," *International Journal of Antennas and Propagation*, **2018**, 2018, p. 3903412.
7. L. Olmi and P. Bolli, "Feasibility Study of Angular Super-Resolution with the Active Surface of a Radio Telescope," 2020 XXXIIIrd General Assembly and Scientific Symposium of the International Union of Radio Science, Rome, Italy, August-September 2020, pp. 1-4.